S1   Calculation of average settling velocity and particle distance

S1.1   Settling velocity

The settling velocity v_t [cm s^{-1}] of a (spherical) aerosol particle with diameter D_p [cm] and density ρ_p (1.05 g cm^{-3}, Section S2.1) can be calculated as

$$v_t = \frac{1}{18} \frac{D_p^2 \rho_p \, g \, C_c}{\mu} \tag{S1}$$

whereas C_c is the dimensionless slip correction factor (Table 9.3 in Seinfeld and Pandis (2006)), g is the acceleration of gravity (9.807 m s^{-2}) and μ is the viscosity 1.72·10^{-4} g cm^{-1} s^{-1} (Equation 9.42 in Seinfeld and Pandis (2006)). Using a global model, (Burrows et al., 2009) estimated the mean atmospheric residence times for CCN active bacteria with equivalent diameters of 1 μm and 3 μm which are indicated in Figure S1.
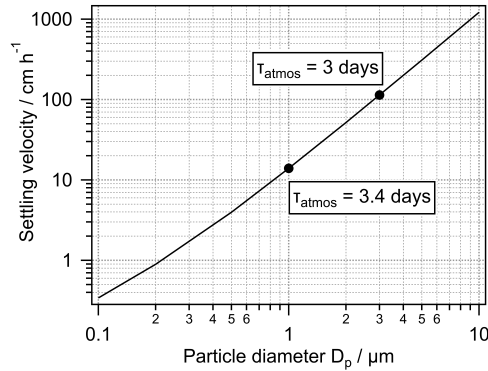
Figure S1. Settling velocity [cm s^{-1}] for spherical aerosol particles with diameter D_d. τ_{atmos} denotes the mean atmospheric residence times for CCN-active bacteria as estimated by Burrows et al. (2009). These numbers are only added for guidance; we do not imply a directly linear relationship between τ_{atmos}, D_p and v_t.

S1.2   Average distance between particles (bacteria cells)

We assume an equidistant distribution of particles (or droplets or bacteria cells) in a cube of air. Figure S2a shows schematically a distribution with a concentration of N = 64 (4 × 4 × 4) particles in a cube with the volume V (side length $V^{1/3}$). The distance δ between neighboring particles is thus

$$\delta = \sqrt[-3]{N} \tag{S2}$$

Figure S2b shows the approximate distance δ [cm] of aerosol particles, cloud droplets and airborne bacteria cells in the atmosphere for the respective typical concentrations N in cm^{-3}.

a) Schematic equidistant distribution in a cube of volume V ($V^{1/3} \times V^{1/3} \times V^{1/3}$)

b) Average distance between bacteria cells, cloud droplets or aerosol particles for typical atmospheric concentrations
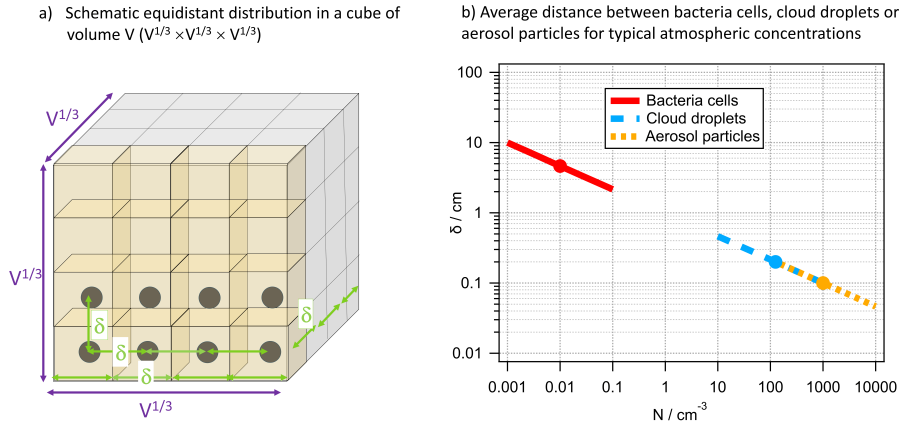
Figure S2. a) Schematic equidistant distribution of particles with a concentration of N in a cube with side length a. The cube can be partitioned into smaller cubes. The distance between the centers of these smaller cubes corresponds to $\sqrt[-3]{N}$; b) average distance δ between bacteria cells, cloud droplets or aerosol particles for their typical atmospheric concentrations N.

S2 Amount of water surrounding airborne bacteria

S2.1 Calculation of $n_{H2O,dr}$ and $l_{H2O,dr}$

A bacteria cell is composed to ~70% of water (e.g., *Nature Scitable*). Assuming a typical cell density of ρ_{cell} = 1.05 g cm^{-3} (1.035 - 1.093) (Bakken and Olsen, 1983), the water mass $m_{cell,H2O}$ inside a cell with an equivalent diameter of $D_{cell} = 10^{-4}$ cm (1 μm) can be calculated as $3.8 \cdot 10^{-13}$ g cell^{-1} according to

$$m_{cell,H2O} = \frac{\pi}{6} D_{cell}^3 \rho_{cell} \cdot 70\% \tag{S3}$$

which corresponds to $1.3 \cdot 10^{10}$ water molecules per cell using

$$n_{cell,H2O} = m_{cell,H2O} \cdot M_{H2O} \cdot N_A \tag{S4}$$

whereas $M_{H2O)}$ is the molecular weight of water (18 g mol^{-1}) and N_A is the Avogadro constant ($6.023 \cdot 10^{23}$ molecules per mole).

Based on the equations by Rose et al. (2008), a relationship between the dimensionless hygroscopic growth factor G and the hygroscopicity parameter κ (Petters and Kreidenweis, 2007) can be derived:

$$a_w = \frac{D_w^3 - D_d^3}{D_w^3 - D_d^3(1 - \kappa)} \tag{S5}$$

Replacing the wet diameter D_w by

$$D_w = G \cdot D_d \tag{S6}$$

one obtains

$$a_w = \frac{G^3 - 1}{G^3 - (1 - \kappa)} \tag{S7}$$

which can then be converted to

$$\kappa = \frac{G^3 - 1}{a_w} - (G^3 - 1) = (G^3 - 1)\left[\frac{1}{a_w} - 1\right] \tag{S8}$$

Using Equation S8 and the growth factors by Lee et al. (2002) and Després et al. (2012), we can derive an (average) $\kappa_{bact} \lesssim$ 0.1 for bacteria under subsaturated conditions (RH < 100%).

Table S1. Hygroscopic growth factors for bacteria as a function of RH based on the study by Lee et al. (2002) and the review by Després et al. (2012).

RH / %	G	κ	
			E coli, Lee et al. (2002)
50	1.05	0.16	
70	1.065	0.1	
90	1.16	0.06	
95	1.32	0.07	
			Various bacteria, Després et al. (2012)
95	1.3	0.07	*Bacillus subtilis*
90	1.22	0.09	*Saccharomonospora viridis*
		0.1	$= \kappa_{av}$; estimate in the present study

To calculate how much water is surrounding the bacteria cells, we convert Equation S8 to

$$G = \sqrt[3]{\frac{a_w \kappa}{1 - a_w} + 1} \tag{S9}$$

Using the growth factors G, we calculate the number of water molecules in the hydration shell as

$$n_{H2O} = \frac{\pi}{6} D_d^3 \cdot (GF^3 - 1) \cdot \frac{\rho_{H2O} N_A}{M_{H2O}} \tag{S10}$$

Based on the schematic in Figure S3 and using Equation S6, the number of water layers may be approximated as (assuming that each layer thickness is the length of water molecule)

$$l_{H2O} = \frac{D_{cell}(G - 1)}{2 \cdot d_{H2O}} \tag{S11}$$

Table S2. Growth factors G for $50\% \leq RH \leq 95\%$ using $\kappa_{bact} = 0.1$ and the corresponding water amount expressed in number of water molecules n_{H2O} (Equation S10) and water layers l_{H2O} (Equation S11). While strictly the concept of hygroscopic growth does not apply at RH > 100%, we also list G values for cloud droplet sizes (i.e. RH $\sim$100%) as the same equations can be applied to calculate n_{H2O} and l_{H2O} based on the water volume.

RH / %	G	n_{H2O} / 10^{10}	l_{H2O}
50	1.03	1.8	59
70	1.07	4.1	132
90	1.24	15.8	434
95	1.32	33.3	775
$\sim$100 ($D_w = 5\ \mu$m)	5	217	7200
$\sim$100 ($D_w = 20\ \mu$m)	20	14000	34500

Growth factor

$$\frac{D_w - D_{cell}}{2}$$

$D_{cell} = 1 \, \mu m$

$D_w = D_{cell} \cdot G$

Single water molecule

$d_{H2O} \sim 2.75 \, Å$
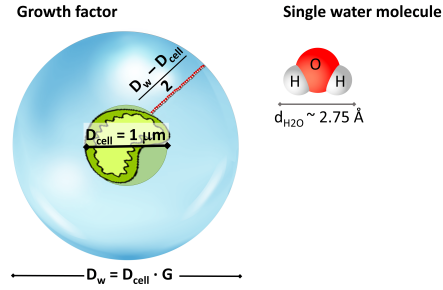
Figure S3. Schematics of a bacteria cell surrounded by water (not to scale) to illustrate how the number of water layer l_{H2O} (Equation S11) is calculated using the size of a water molecule of 2.75 Å (10^{-10} m)

S2.2 Droplet lifetime τ_{cloud}

Cloud droplets form near cloud base where the water vapor saturation reaches values of > 1. The number of cloud droplets (= activated cloud condensation nuclei) depends on the supersaturation, which, in turn, is a function of the updraft velocity w [m s^{-1}] (proportional to the cooling rate) and the concentration of droplets on which water vapor can condense (condensational sink). Cloud droplets grow while they are lifted towards cloud top across the cloudy layer (= cloud thickness δ_{cloud} [m]). Eventually evaporational cooling causes air parcels to descend, leading to downward motion (downdraft, -w) during which the droplets shrink. The time scale of the life cycle of a cloud droplet can be, thus, approximated as

$$\tau_{dr} \simeq 2 \cdot \frac{\delta_{cloud}}{|w|} \tag{S12}$$

This cycle is illustrated in Figure S4a; in panel Figure S4b the results of Equation S12 are shown with the grey square indicating the typical range of δ_{cloud} and w for stratocumulus clouds, the most abundant clouds on Earth. The figure shows a range of 10 min $\lesssim \tau_{cloud} \lesssim$ 30 min. This value may be even valid for other (e.g., more convective) cloud types that usually exhibit higher updraft velocities and greater thickness.
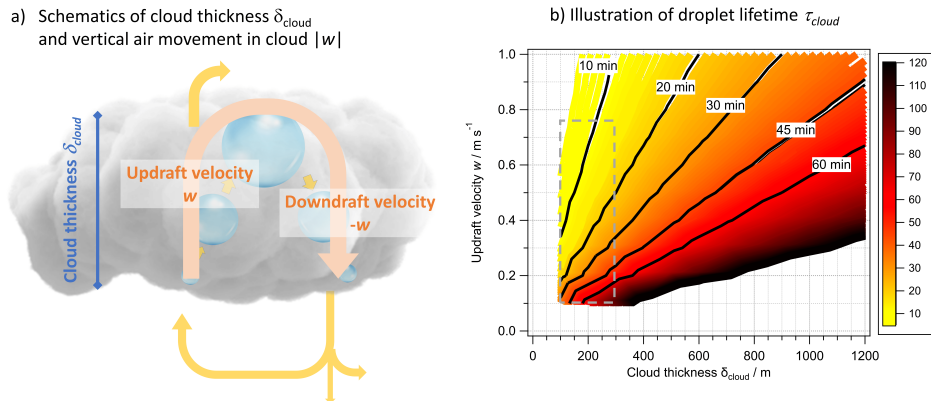
Figure S4. a) Schematics of vertical air movement in clouds of thickness δ_{cloud}; air may cycle multiple times through a cloud but these cycles are always interrupted by periods at which the particle encounters RH < 100%. b) Cloud droplet lifetimes as a function of cloud thickness δ_{cloud} and updraft velocity w (Equation S12). They grey square denotes the approximate δ_{cloud}-w range for stratocumulus clouds (e.g., Rogers and Yau (1996)). The figures shows that individual cloud droplets exist for $\sim$10 - 30 min.

S3 Concentration ratio of solutes (e.g. organic nutrients) per cell

The concentration of organic compounds in surface waters has been measured in numerous studies. A small collection of such studies is summarized in Table S3. We selected studies that focused on biodegradation implying that the target organics are those that serve as nutrients for bacteria.

Table S3. Selected studies that reported concentrations of small organic compounds in surface waters together with bacteria cell concentrations. All these studies discussed the biodegradation of the organics in the aquatic environments.

Organic compound	[Org] / (μmol L^{-1})	[Cells] / mL^{-1}	log([Org]/[Cell] / (mol cell^{-1})	Environment	Reference
LMW [1]	26 - 84 (52) [2]	$6 \cdot 10^6$ - $8.5 \cdot 10^6$ ($7 \cdot 10^6$)	-8.1	Intermittent river	Catalán et al. (2017)
Ethanol	0.089 [3]	1 - 306 (70)	-4.7	Coastal seawater	de Bruyn et al. (2020)
Acetaldehyde	0.372	350 - 31100 (5100)	-6.4	Coastal seawater	de Bruyn et al. (2017)
Methanol	0.08 - 0.3 (0.2)	$0.33 \cdot 10^5$ - $0.87 \cdot 10^5$ ($7 \cdot 10^5$)	-9.9	Tropical Atlantic	Dixon et al. (2011)
Acetone	0.005 - 0.1 (0.06)	5000	-9.9	Coastal seawater	de Bruyn et al. (2013)

[1] Low molecular weight fraction

[2] The original numbers were given in mg L^{-1}; we converted them assuming a molecular weight of 100 g mol^{-1}

[3] This concentration was used in lab experiments; adjusted to previously measured sea water concentration.
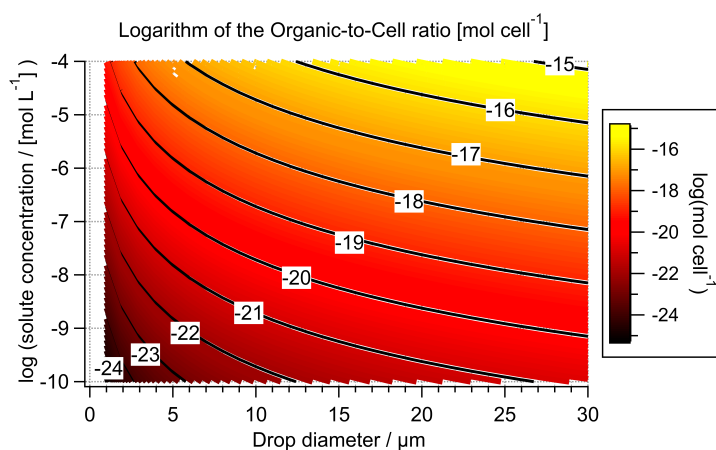
Figure S5. Illustration of the solute-to-cell ratio (logarithm) in a single cloud droplet as a function of drop diameter and solute concentration (Equation S13). The numbers along the contour lines denote the logarithm of the ratio as also shown in the color scale.

The range of (organic) solute concentrations in cloud water is $\sim 10^{-10}$ - 10^{-4} moles per liter, depending on the solubility and total (gas +aqueous) concentration of the solute. The number of moles solute in a single droplet with diameter D_{dr} [cm] as a function of solute concentration $[Sol]_{aq}$ (in moles per liter) is

$$n_{sol,dr} = \frac{\pi}{6} D_{dr}^3 \cdot [Sol]_{aq} \cdot 10^{-3} \, L \, cm^{-3} \tag{S13}$$

Assuming that the cell concentration per droplet is 1, the organic-to-cell ratio (in moles per cell) is

$$\frac{[Org]}{[Cell]} = \frac{n_{sol,dr} \, (moles \, droplet^{-1})}{1 \, (cell \, droplet^{-1})} \tag{S14}$$

Figure S5 shows the resulting ratios as a function of drop diameter and bulk solute concentration.

S4 OH radical concentration and production rates in cloud droplets

The average number of OH radicals in a droplet with diameter D_{dr} [cm] is calculated as

$$n_{OH,dr} = \frac{\pi}{6} D_{dr}^3 \cdot [OH]_{aq} \cdot N_A \cdot 10^{-3} \, L\,cm^{-3} \tag{S15}$$

whereas $[OH]_{aq}$ is the bulk OH concentration in moles per liter aqueous phase. OH in cloud droplets can be produced by several reactions in cloud droplets, including those listed in Table S4. Accordingly, the production of OH radicals in a single droplet can be calculated based on model-derived source rates R_{aq} [mol L^{-1} s^{-1}]

$$R_{OH,dr} = \frac{\pi}{6} D_{dr}^3 \cdot R_{aq} \cdot N_A \cdot 10^{-3} \, L\,cm^{-3} \tag{S16}$$

Table S4. Major pathways that lead to OH formation in cloud droplets; reactant concentrations are taken from (Barth et al., 2021), rate constants are from the 'Ervens model' in the same study.

Reaction	Reactant concentrations / (μmol L^{-1})	k	R_{aq} / (10^{-10} mol L^{-1} s^{-1})
$H_2O_2 + h\nu \rightarrow 2\,OH$	$[H_2O_2] \sim 100$	10^{-6} s^{-1}	2
$NO_3^- + h\nu\,(+ H_2O) \rightarrow NO_2 + OH$	$[NO_3^-] \sim 100$	10^{-7} s^{-1}	0.2
$Fe^{2+} + H_2O_2 \rightarrow Fe^{3+} + OH^- + OH$	$[Fe^{2+}] \sim 1$	55 L mol^{-1} s^{-1}	55
$O_3 + O_2^- \rightarrow 2\,O_2 + OH$	$[O_3] \sim 0.0005$, $[O_2^-] \sim 0.002$	$1.5 \cdot 10^9$ L mol^{-1} s^{-1}	15
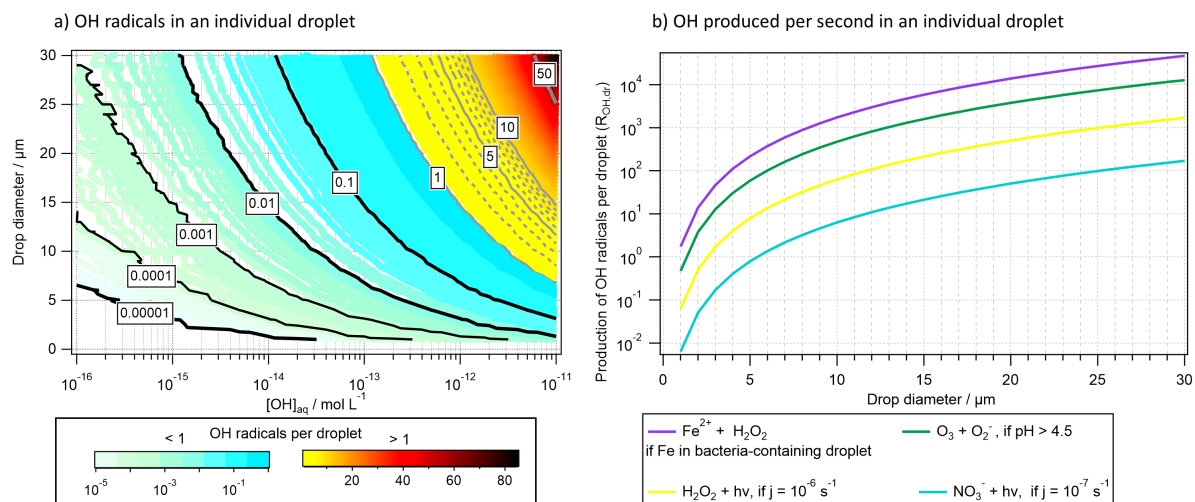
Figure S6. a) The contour lines indicate the number of OH radicals in a single droplet ($n_{OH,dr}$, Equation S15) as a function of the bulk aqueous phase concentration [OH]$_{aq}$ and drop diameter D_{dr}. The two color scales distinguish the regime when the steady-state OH concentration is less or greater than one OH radical per droplet (< 1; > 1), respectively; b) number of OH radicals produced per second in a droplet ($R_{OH,dr}$, Equation S16) by individual chemical OH sources inside a droplet. These numbers are calculated using the values in Table S4

References

Bakken, L. R. and Olsen, R. A.: Buoyant densities and dry-matter contents of microorganisms: conversion of a measured biovolume into biomass., Applied and environmental microbiology, 45, 1188–1195, https://doi.org/10.1128/aem.45.4.1188-1195.1983, 1983.

Barth, M. C., Ervens, B., Herrmann, H., Tilgner, A., McNeill, V. F., Tsui, W. G., Deguillaume, L., Chaumerliac, N., Carlton, A., and Lance, S. M.: Box Model Intercomparison of Cloud Chemistry, Journal of Geophysical Research: Atmospheres, 126, e2021JD035 486, https://doi.org/10.1029/2021JD035486, 2021.

Burrows, S. M., Butler, T., Jöckel, P., Tost, H., Kerkweg, A., Pöschl, U., and Lawrence, M. G.: Bacteria in the global atmosphere – Part 2: Modeling of emissions and transport between different ecosystems, Atmospheric Chemistry and Physics, 9, 9281–9297, https://doi.org/10.5194/acp-9-9281-2009, 2009.

Catalán, N., Casas-Ruiz, J. P., von Schiller, D., Proia, L., Obrador, B., Zwirnmann, E., and Marcé, R.: Biodegradation kinetics of dissolved organic matter chromatographic fractions in an intermittent river, Journal of Geophysical Research: Biogeosciences, 122, 131–144, https://doi.org/10.1002/2016JG003512, 2017.

de Bruyn, W. J., Clark, C. D., Pagel, L., and Singh, H.: Loss rates of acetone in filtered and unfiltered coastal seawater, Marine Chemistry, 150, 39–44, https://doi.org/10.1016/j.marchem.2013.01.003, 2013.

de Bruyn, W. J., Clark, C. D., Senstad, M., Barashy, O., and Hok, S.: The biological degradation of acetaldehyde in coastal seawater, Marine Chemistry, 192, 13–21, https://doi.org/10.1016/j.marchem.2017.02.008, 2017.

de Bruyn, W. J., Clark, C. D., Senstad, M., Toms, N., and Harrison, A. W.: Biological degradation of ethanol in Southern California coastal seawater, Marine Chemistry, 218, 103 703, https://doi.org/10.1016/j.marchem.2019.103703, 2020.

Després, V. R., Huffman, J. A., Burrows, S. M., Hoose, C., Safatov, A. S., Buryak, G., Fröhlich-Nowoisky, J., Elbert, W., Andreae, M. O., Pöschl, U., and Jaenicke, R.: Primary biological aerosol particles in the atmosphere: a review, Tellus B, 64, 15 598, https://doi.org/10.3402/tellusb.v64i0.15598, 2012.

Dixon, J. L., Beale, R., and Nightingale, P. D.: Rapid biological oxidation of methanol in the tropical Atlantic: significance as a microbial carbon source, Biogeosciences, 8, 2707–2716, https://doi.org/10.5194/bg-8-2707-2011, 2011.

Lee, B. U., Kim, S. H., and Kim, S. S.: Hygroscopic growth of E. coli and B. subtilis bioaerosols, J. Aerosol Sci., 33, 1721–1723, https://doi.org/10.1016/S0021-8502(02)00114-3, 2002.

Petters, M. D. and Kreidenweis, S. M.: A single parameter representation of hygroscopic growth and cloud condensation nucleus activity, Atmospheric Chemistry and Physics, 7, 1961 – 1971, https://doi.org/10.5194/acp-7-1961-2007, 2007.

Rogers, R. R. and Yau, M. K.: A Short Course in Cloud Physics, Elsevier Science, Burlington, MA, 3rd edn., 1996.

Rose, D., Gunthe, S. S., Mikhailov, E., Frank, G. P., Dusek, U., Andreae, M. O., and Pöschl, U.: Calibration and measurement uncertainties of a continuous-flow cloud condensation nuclei counter (DMT-CCNC): CCN activation of ammonium sulfate and sodium chloride aerosol particles in theory and experiment, Atmospheric Chemistry and Physics, 8, 1153–1179, https://doi.org/10.5194/acp-8-1153-2008, 2008.

Seinfeld, J. H. and Pandis, S. N.: Atmospheric Chemistry and Physics - From air pollution to climate change, John Wiley & Sons, Inc., Hoboken, New Jersey, 2nd edn., 2006.